ACS Combinatorial Science

Research Article

pubs.acs.org/acscombsci

Hydrogen Storage Materials Discovery via High Throughput Ball Milling and Gas Sorption

Bin Li, Steven S. Kaye, Conor Riley, Doron Greenberg, Daniel Galang, and Mark S. Bailey*

Wildcat Discovery Technologies, Inc., San Diego, California 92121, United States

Supporting Information

ABSTRACT: The lack of a high capacity hydrogen storage material is a major barrier to the implementation of the hydrogen economy. To accelerate discovery of such materials, we have developed a high-throughput workflow for screening of hydrogen storage materials in which candidate materials are synthesized and characterized via highly parallel ball mills and volumetric gas sorption instruments, respectively. The workflow was used to identify mixed imides with significantly enhanced absorption rates relative to $Li_2Mg(NH)_2$. The most promising material, $2LiNH_2$:MgH_2 + 5 atom % $LiBH_4$ + 0.5 atom % La, exhibits the best balance of absorption rate, capacity, and cycle-life, absorbing >4 wt % H_2 in 1 h at 120 °C after 11 absorption-desorption cycles.

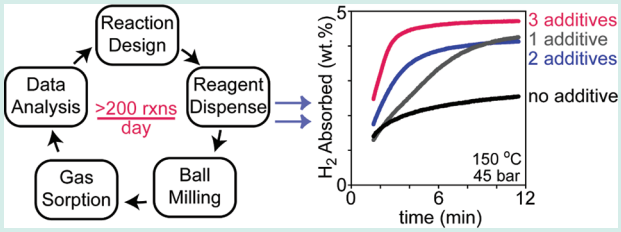

KEYWORDS: *high-throughput, hydrogen storage, ball milling, mechanochemistry, gas sorption, amides*

INTRODUCTION

Improved hydrogen storage materials are required to enable the hydrogen economy.[1−3] For use in mobile applications, potential storage materials must exhibit high capacity, rapid rate and reversible sorption under reasonable operating conditions ($-40 < T < 85$ °C; $3 < P < 100$ bar for automobiles[4]) for thousands of cycles. Although the hydrogen storage properties of a wide variety of systems have been studied (e.g., metal−organic frameworks (MOFs), intermetallics, and complex hydrides), no known material meets the required performance criteria.[1,3] For example, although MOFs exhibit high capacity and rapid sorption rates, significant uptake can only be obtained at cryogenic temperatures; intermetallics exhibit rapid absorption under moderate conditions but have low capacity; and complex hydrides operate only at elevated temperatures because of large activation energies. Although new materials must be discovered, the need to tune both the thermodynamics and the kinetics of the material-hydrogen interaction and to identify a highly efficient cycling material necessitates the search of a dauntingly large chemical space.

High throughput tools and methods have proven successful in the discovery of a wide array of complex materials including phosphors, dielectric materials, and catalysts.[5,6] Because of this success, groups have begun to develop high throughput approaches to hydrogen storage including computational screening methodologies to identify reactions with suitable thermodynamics.[7,8] In addition, Moleski et al.,[9] Griessen et al.,[10,11] Smith et al.,[12] Amieiro-Fonseca et al.[13] Barcelo and Mao,[14] Bendersky et al.,[15] and Downing et al.[16] have reported high throughput studies of the hydrogen storage properties of thin films; however, this work is yet to be extended to high-throughput screening of bulk powders, the form factor necessary for automotive applications. Lewis et al. reported the development of a parallel gas sorption instrument capable of testing 48 samples at a time and its use to identify improved sorption kinetics in the $Li_2Mg(NH)_2$ system.[17] However, samples are not prepared in a high throughput fashion. In conferences, Zhao and Lemmon have presented a hydrogen storage workflow; however, the exact capabilities are not published.[18] Our workflow described herein builds upon these results by incorporating parallel gas sorption instruments and parallel ball mills into a complete high throughput workflow capable of synthesizing and analyzing >200 powder samples per day. The workflow incorporates reaction design, automated reagent dispensing, ball milling, volumetric gas sorption measurements, reaction quenching, and data analysis. Ball milling can be performed under inert or reactive atmospheres (e.g., He or H_2) within a variety of reaction containers (ceramic, metal, plastic) capable of withstanding 150 bar and with control of all key variables in the milling process such as acceleration, time, and ball:powder ratio. The gas sorption instruments can operate at pressures and temperatures of 67 bar and 160 °C and are able to measure hydrogen absorption and desorption as a function of time, pressure, and temperature.

Ball milling was selected as our synthesis method because it can be used to synthesize a wide variety of materials including alloys, intermetallics, semiconductors, and ceramics.[19−23] For example, hydrogen storage materials,[24] electrode materials for lithium ion batteries,[25,26] catalysts for PEM fuel cells,[27] and thermoelectric materials[28] have all been synthesized by ball-milling. Furthermore, milling produces powder consisting of small particles and crystallites with a high concentration of

Received: October 27, 2011
Revised: March 9, 2012
Published: May 22, 2012

   dx.doi.org/10.1021/co2001789 | ACS Comb. Sci. 2012, 14, 352−358

rapid diffusion regions (e.g., grain boundaries, defects) ideal for rapid sorption kinetics. Additionally, the intimate mixing achieved within the powder is ideal for any necessary subsequent thermal processing to increase crystallinity or engender further reaction. In addition, in contrast to currently employed solution-based high throughput synthesis techniques, ball-milling is a solid-state approach that can produce materials in high yield from typically simple (often elemental) reagents, necessitating little, if any, workup. Indeed, the potential of ball milling to drive chemical reactions (organic or inorganic) in the absence of solvent may lead to more sustainable syntheses.[29] High-pressure volumetric gas sorption was chosen as our measurement technique because it can provide direct measures of absorption and desorption phenomena as a function of time, temperature, and pressure, from which both the sorption enthalpy and activation energy can be extracted. In contrast to optical measurements of reaction heat, gas sorption provides a direct measure of the capacity of the material and is equally suited to powdered materials or thin-films. Gravimetric analyses were not pursued because the necessary buoyancy correction to the obtained data requires knowledge of sample density, a material-specific parameter that will often not be known prior to measurement.

The mixed imide, $Li_2Mg(NH)_2$, is one of the most promising hydrogen storage materials,[30,31] and is the first system studied by our tools. It absorbs significant amounts of hydrogen (5.6 wt %) according to the following reaction

$$Li_2Mg(NH)_2 + 2H_2 = 2LiH + Mg(NH_2)_2 \quad (1)$$

with absorption thermodynamics corresponding to an equilibrium hydrogen pressure of approximately 1 bar at 90 °C (ΔH = −44 kJ [mol H_2]$^{-1}$; ΔS = −112 J [K·mol H_2]$^{-1}$),[32] close to the operating temperature of a polymer exchange membrane fuel cell. However, slow absorption and desorption rates preclude use of this material. For example, Luo et al. reported in 2007 that $Li_2Mg(NH)_2$ absorbs only 60% of its total capacity in 5 h at 200 °C and under 110 bar H_2 pressure.[33] Since the initial report of the $Li_2Mg(NH)_2$ system, the kinetics of reaction 1 have been improved by reducing the reactant particle size via ball milling[34] and through the addition of various compounds and mixtures (generally, additives). The first reported additive was $LiBH_4$, which was identified via a high-throughput screen of the $LiNH_2$−MgH_2−$LiBH_4$ phase space.[17,35] In this research, Lewis et al. synthesized and screened a total of 66 reactions, identifying $2LiNH_2$:$1MgH_2$:1/3$LiBH_4$ as the composition with the best reversibility and kinetics. Yang and co-workers studied the composition $2LiNH_2$:$1MgH_2$:$1LiBH_4$, characterizing the reaction pathway and confirming that the addition of $LiBH_4$ significantly enhances the observed absorption and desorption rate.[36] Subsequent fine-tuning of the optimal $LiNH_2$:MgH_2:$LiBH_4$ ratio was performed,[37,38] leading to the identification of $2LiH$:$1Mg(NH_2)_2$:$0.1LiBH_4$ (i.e., 3 at.% $LiBH_4$) as the optimal composition in this pseudoternary system, exhibiting initial desorption and absorption rates three times that of the system without any additive.[37] Chen et al. further demonstrated that equivalent hydrogen storage properties were observed from ball-milled mixtures of LiH−$Mg(NH_2)_2$−$LiBH_4$ and $LiNH_2$−MgH_2−$LiBH_4$.[39] In addition to $LiBH_4$, further additives have been identified; for example, the dehydrogenation rate has been increased via the addition of excess $Li_2Mg(NH)_2$,[40] Li_3N,[41] or $NaBH_4$.[42] Furthermore, the absorption and desorption rates have been enhanced via, for example, graphite-supported ruthenium nanoparticles,[43] triphenyl phosphate,[44] and significantly by ZrCo: upon addition of ZrCo, $Li_2Mg(NH)_2$ absorbs ∼5 wt % in 20 min at elevated temperatures and pressures (150 °C/70 bar).[45] However, to date, partial substitution of KH for LiH produces a material with the fastest reported rate of hydrogen sorption under moderate conditions.[46] Chen et al. reported that ball-milled mixtures of 0.1KH:1.9LiH:1Mg-$(NH_2)_2$ absorb 4.2 wt % H in 15 min at 143 °C and 30 bar.

Herein we report a high-throughput screen of additives in the $Li_2Mg(NH)_2$ system. Our study is motivated by the high capacity and reversibility of $Li_2Mg(NH)_2$, and the wide range of chemically distinct additives that induce improvements in sorption kinetics. Our goal was to 1) demonstrate our high throughput workflow by screening the effect of a wide variety of additives upon the absorption rate of $Li_2Mg(NH)_2$ and 2) to identify materials with high capacity and increased absorption rate under moderate conditions. The most promising material identified, $2LiNH_2$:MgH_2 + 5 atom % $LiBH_4$ + 0.5 atom % La, absorbs >4 wt % H_2 in 1 h at 120 °C even after 11 absorption-desorption cycles.

RESULTS AND DISCUSSION

Our goal was to increase the absorption rate of the $Li_2Mg(NH)_2$ system (reaction 1), with minimal impact on overall capacity. As noted above, additives are known to enhance the kinetics of reaction 1; therefore, the initial phase of our research was a systematic screen of large numbers of potential additives and combinations of additives including elements, compounds, and supported metal catalysts for absorption rate enhancement. The additives were selected according to the following strategies. The effect of doping (both iso- and aliovalent) of the metal sites was probed through the addition of electropositive metals such as sodium, calcium and aluminum with similar ionic radii to lithium and magnesium. Excess amounts of lithium and magnesium were also tested. Catalytic metals such as ruthenium have been shown to improve the sorption rate in this system;[43] therefore, we selected a broad array of transition metals and supported transition metal nanoparticles to optimize this effect. Both the potential metal dopants and catalysts were added as elements and as compounds to test the effect of the reagent used (e.g., Na/NaH/$NaBH_4$, Pd/supported palladium nanoparticles and Ti/TiH_2/$TiCl_3$). In addition, the potential to destabilize[47] reaction 1 was assessed through the addition of complex metal hydrides and metal nitrides such as $NaAlH_4$ and Mg_3N_2. Sorption rate enhancement has been induced in $Li_2Mg(NH)_2$ and other hydrogen storage materials through particle size reduction,[34,48,49] suggesting that strategies to optimize particle size and morphology would also be fruitful. The particle size and morphology induced by ball milling can be strongly dependent upon process control agents (PCAs).[19−21] PCAs are additives introduced in small amounts during ball milling (typically 1−5 wt %) that effect significant changes in the resultant material morphology. Although not completely understood, the effect is likely due to processes such as surface stabilization, inhibition of particle agglomeration, or enhanced grinding of the materials. We therefore selected a number of additives different in chemical and mechanical properties such as graphite, mesoporous carbon, silicon, boron, and metal oxides to test the effects of PCAs in this system. The additives chosen are summarized in Table 1. Some additives may enhance the performance via multiple routes (e.g., Ti may dope

dx.doi.org/10.1021/co2001789 | ACS Comb. Sci. 2012, 14, 352−358

Table 1. Summary of the Additives Tested and the Rationale for Their Choice

dopants	Li, Na, Mg, Ca, B, Al
	LiH, NaH, KH, CaH_2
destabilizers	$LiBH_4$, $NaBH_4$, $LiAlH_4$, $NaAlH_4$, Li_3N, Mg_3N_2, NH_3BH_3
catalysts	Pd, C_Pd, C_Pt, C_Ru, Ti, TiH_2, Zr, V, Cr, Mn, Fe, Co, Ni, Cu, Zn, $LaNi_5$
	YCl_3, $LaCl_3$, $TiCl_3$, VCl_3, $CrCl_2$, $CrCl_3$, $FeCl_3$, $NiCl_2$, CuCl, $CuCl_2$, $ZnCl_2$
PCAs	Darco, Graphite, Si (300 μm), Si (100 nm), Y, La
	Y_2O_3, La_2O_3, CeO_2, ZrO_2, Nb_2O_5, Al_2O_3

on the metal site, or act as a catalyst); however, for clarity we have listed each additive only once.

The performance of the materials was assessed with our primary screen. Since reaction 1 is known to be reversible, the primary screen measured only the first cycle sorption kinetics:[50] once the synthesized materials were desorbed, hydrogen absorption at 150 °C was measured by exposing the materials to about 45 bar hydrogen for 30 min. The amount absorbed in 30 min is indicative of the absorption rate of the material and used as the primary metric in this screen. This approach was validated by replicating the high-throughput screen of the $LiNH_2$−MgH_2−$LiBH_4$ phase space reported by Lewis et al.[17] Sixty-six reactions within the pseudoternary phase space xLiNH$_2$ + yMgH$_2$ + zLiBH$_4$ (x, y, z = 0, 0.1, 0.2, ..., 0.9, 1; x + y + z = 1) were synthesized and tested using our approach, yielding excellent agreement with that reported by Lewis et al. (Supporting Information, Figure. S1). Once validated, the primary screen was used to assess the effect of all the selected additives upon the absorption rate of the Li−Mg−N−H system. As an example of the data obtained, shown in Figure 1

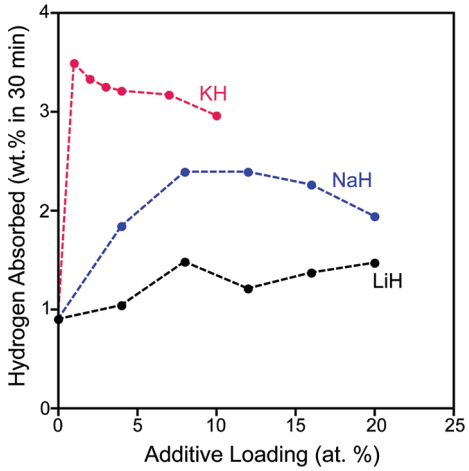

Figure 1. Measured 30 min hydrogen absorption for selected ternary systems. The systems are of the form 2LiNH$_2$:MgH$_2$ + Additive. Hydrogen absorbed is wt % of the total loaded reagent mass; that is, mass H_2 absorbed/(mass of 2LiNH$_2$ + MgH$_2$ + xA). Dashed lines are guides to the eye.

is the 30 min absorption obtained for one family of materials, 2LiNH$_2$ + 1MgH$_2$ + xMH (M = Li, Na, K). The largest rate enhancement was observed with KH, though all of the alkali hydrides led to an improvement in the measured absorption rate (as measured by the uptake in 30 min). It is interesting to note that, although we observe a rate enhancement upon KH addition consistent with Chen et al.[46] we observe a smaller amount of hydrogen absorbed within the first 30 min. Chen et al. reports a 30 min capacity at 143 °C of ∼4.7 wt % for 0.1KH:1.9LiH:1Mg$(NH_2)_2$, approximately 1 wt % (1 H atom per formula unit) more than the maximum uptake we observe at 150 °C in the primary screen or after complete absorption at 120 °C (see below). The observed difference in capacity likely results from differences in stoichiometry arising from addition rather than substitution of KH.

To illustrate the effect of all the combinations tested, we plot in Figure 2 the maximum observed 30 min uptake for each system, 2LiNH$_2$ + MgH$_2$ + xA (see Supporting Information, Figure S2 for a more detailed illustration). Two important effects are observed. First, a broad range of hydrogen absorption is observed, indicating that additives have a significant effect on the absorption rate of reaction 1. Second, materials made from a wide variety of additives selected through many of the strategies outlined above exhibit enhanced absorption rates. Examples include 2LiNH$_2$ + MgH$_2$ + xA, A = KH, NaH, $LiBH_4$, Li_3N, V, Pd, supported palladium nanoparticles (C_Pd), ZrO_2, and CeO_2. Although further analysis is required to determine why these materials exhibit improved absorption kinetics, we speculate that a number of different mechanisms are responsible for the enhanced absorption rates observed in these materials. Additional observations of note include: Darco (a commercial mesoporous carbon) induces a greater absorption rate than graphite; of the 3d transition metals, only titanium, vanadium, and nickel were found to be effective; both 300 μm and 50 nm silicon powder enhance the observed rate; palladium and all the tested supported metal catalysts lead to enhanced absorption rates, consistent with previous work.[43] It is noted that components with the potential to absorb hydrogen (e.g., V, La, Li) under the reaction conditions were screened. Based upon the maximum theoretical hydrogen capacity of these additives (e.g., LiH, LaH_2, VH_2), their maximum contribution to the primary screen signal shown in Figure 2 is less than 1 wt % ranging from ∼0.3 wt % H (La) to 0.8 wt % H (V) and 0.9 wt % H (Li). Lithium nitride is an exception, in the quantities used (≤20 at. %/27 wt %) it could account for the entire signal (≤2.7 wt % H). However, the rate enhancement induced by Li_3N addition was sustained over many cycles (see below and ref 41), suggesting that the observed primary screen signal is not due to absorption by pure Li_3N, which is irreversible under the assay conditions.

Based upon our hypothesis that a number of different mechanisms were responsible for the observed rate enhancements, secondary libraries were designed based upon quaternary systems including pairs of additives. From Figure 2, it can be seen that the ternary composites containing $LiBH_4$ or KH exhibit the fastest absorption rates, suggesting that both $LiBH_4$ and KH should be used in further screening. However, further analysis (see below) demonstrated that materials containing $LiBH_4$ exhibited superior capacity than those containing KH; therefore, we focused primarily upon combinations of $LiBH_4$ with a second component; for example, 2LiNH$_2$:MgH$_2$ + 10 atom % $[(1 - y)\text{A} + y\text{LiBH}_4]$. For each pair, both the total amount of each component and the relative concentration of each additive within the pair were varied. For the majority of the additive-pairs tested, a quaternary composition was found that absorbed hydrogen faster than ternary compositions containing either of the individual additives (Figure 3 and Supporting Information, Figure S3). An exception is the additive pair $LiBH_4$−Pd, which was found to perform worse than with either additive alone.

dx.doi.org/10.1021/co2001789 | ACS Comb. Sci. 2012, 14, 352−358

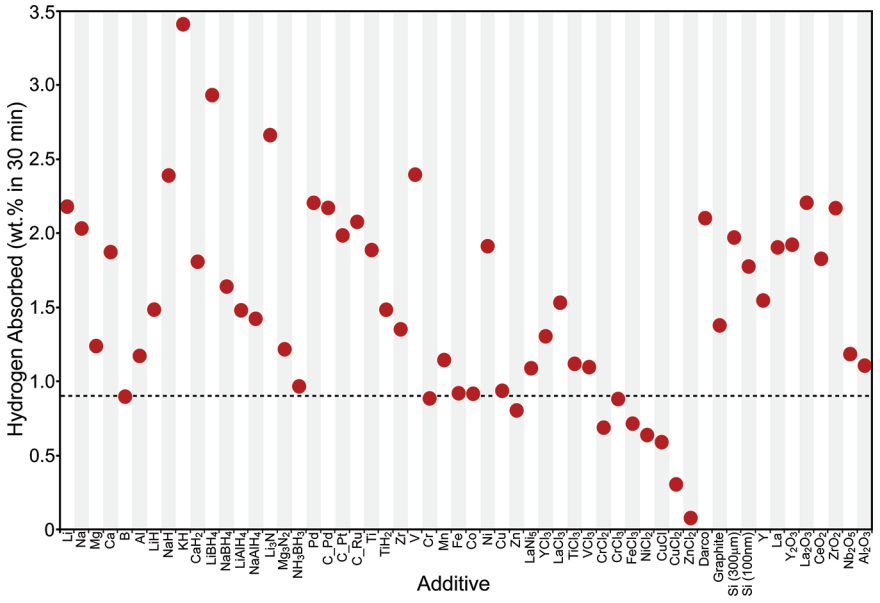

Figure 2. Maximum primary screen uptake for each family of reactions, $2LiNH_2 + MgH_2 + xA$ (A = Additive). The dashed line indicates the measured uptake for $2LiNH_2$:MgH_2 ball-milled under identical conditions. Hydrogen absorbed is wt % of the total loaded reagent mass; that is, mass H_2 absorbed/(mass of $2LiNH_2 + MgH_2 + xA$). More details (uptake vs composition) are shown in Supporting Information, Figure S2.

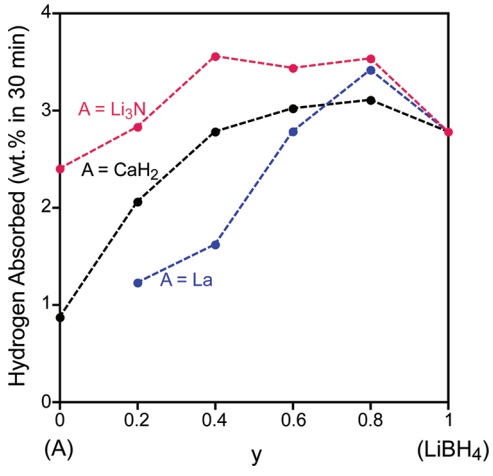

Figure 3. Measured 30 min absorption of selected quaternary systems. The systems are of the form $2LiNH_2$:MgH_2 + 10 atom % $[(1 - y)A + yLiBH_4]$ (A = La, CaH_2, Li_3N). A summary of all systems tested are detailed in Supporting Information, Figure S3. Hydrogen absorbed is wt % of the total loaded reagent mass; that is, mass H_2 absorbed/(mass of $2LiNH_2 + MgH_2 + xA$). Dashed lines are guides to the eye.

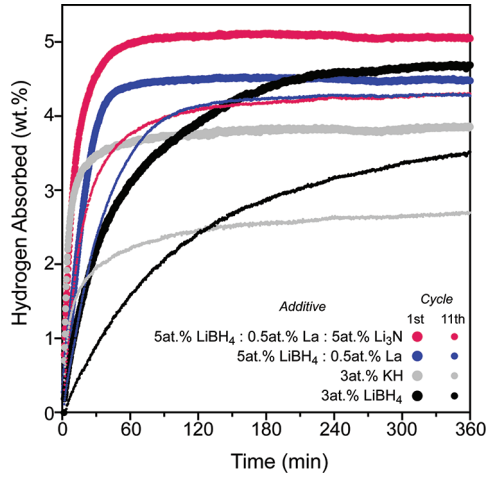

Figure 4. First- and eleventh-cycle isothermal hydrogen absorption at 120 °C and about 45 bar. All reactions are of the form, $2LiNH_2$:MgH_2 + additive(s) and the additives are detailed in the figure. On first cycle, $2LiNH_2$:MgH_2 absorbs 2.4 wt % in 6 h. Hydrogen absorbed is wt % of the total loaded reagent mass; that is, mass H_2 absorbed/(mass of $2LiNH_2 + MgH_2 + xA$).

As a collection of ternary and quaternary systems with enhanced initial absorption rates were identified via the primary screen, the characterization focus shifted toward the determination of which additive or additive combination produced a material with the best balance of rate, capacity, and cycle-life. Eleven cycles of complete uptake measurements (6 h, 120 °C, 45 bar) were performed (Figure 4 and 5, Table 2). Between each absorption measurement, the samples were degassed for 15 h at 140 °C. On the first cycle, the pentenary system incorporating the additives $LiBH_4$, La, and Li_3N, and the ternary system made with KH exhibit the fastest initial uptake (more detail in Supporting Information, Figure S4 and S5). However, both systems exhibit a significant loss in capacity over the eleven cycles: 14 and 31%, respectively. The sample $2LiNH_2$:MgH_2+3 atom %$LiBH_4$ exhibits good initial capacity but relatively slow initial uptake kinetics. These uptake kinetics fade over cycling, resulting in an eleventh-cycle capacity of 3.5 wt %, representing an apparent 25% loss in capacity. However, we note that the material is still absorbing hydrogen at the end of the measurement and the eleventh-cycle absorption capacity of the material would likely increase if the measurement were extended beyond 6 h. In contrast, $2LiNH_2$:MgH_2 + 5 atom % $LiBH_4$ + 0.5 atom %La, exhibits good initial uptake, high capacity, and maintains 96% of its initial capacity after 11 cycles. This is, to our knowledge, the best reported combination of properties in this system under these conditions, and the first report of lanthanum as an additive.

Initial electron micrographs of $LiNH_2$−MgH_2−Li_3N−$LiBH_4$−La indicate the presence of lanthanum-rich sub-300 nm particles dispersed evenly throughout the material

dx.doi.org/10.1021/co2001789 | ACS Comb. Sci. 2012, 14, 352−358

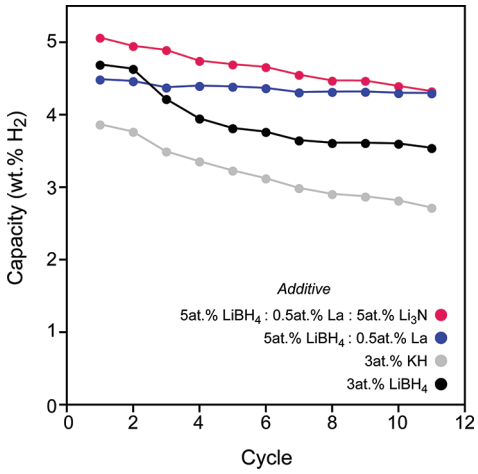

Figure 5. Capacity at 120 °C and 45 bar as a function of cycle life. All reactions are of the form, $2LiNH_2$:MgH_2 + additive(s) and the additives are detailed in the figure. The quaternary material $2LiNH_2$ + MgH_2 + 5 atom % $LiBH_4$ + 0.5 atom %La exhibits only a 4% loss in capacity after 11 cycles. Absorption duration was 6 h; desorption, 15 h (140 °C, dynamic vacuum). Hydrogen absorbed is wt % of the total loaded reagent mass; that is, mass H_2 absorbed/(mass of $2LiNH_2$ + MgH_2 + xA).

Table 2. Summary and Comparison of the Hydrogen Storage Properties of Materials Reported Herein[a]

	cycle life capacity (wt %)			time to 50% capacity (min)	
additives	1st	11th	loss	1st	11th
5%$LiBH_4$ 0.5% La	**4.5**	**4.3**	**4%**	**14**	**26**
5% $LiBH_4$ 1% La 5% Li_3N	5.0	4.3	14%	7	13
3% KH	3.9	2.7	31%	4	8
3% $LiBH_4$	4.7	3.5	25%	37	70

[a]Additive percentages are atomic percent.

(Supporting Information, Figure S7). Complete quantification of the lanthanum-rich particles or the distribution of lanthanum throughout the material via EDS is precluded by the small particle size and the low-energy X-ray emission of hydrogen, nitrogen, and lithium. We note that lanthanum likely does not remain in the elemental form upon synthesis or assay, potentially forming lanthanum hydride (irreversible under the analysis conditions), lanthanum nitride, or other compounds. While further work is required to fully understand the mechanism, we suggest two hypotheses: lanthanum (or a lanthanum containing compound) acts as a PCA in this system to create a powder morphology more suited to hydrogen absorption; and/or, low levels of lanthanum are incorporated into a nonstoichiometric mixed imide with enhanced sorption rates relative to $Li_2Mg(NH)_2$. $Li_2Mg(NH)_2$ is known to accommodate a large number of defects, and it has been shown that vacancies strongly influence the hydrogen storage properties of amide/imide systems.[51,52]

CONCLUSION

We have screened >50 additives and successfully identified a material, $2LiNH_2$:$1MgH_2$ + 5 atom % $LiBH_4$ + 0.5 atom % La, with an improved balance of kinetics, capacity, and cycle life for hydrogen uptake. In addition, we have identified a number of elements such as silicon and lanthanum whose ability to enhance the absorption rate of $Li_2Mg(NH)_2$ is surprising and may not have been identified via traditional approaches. Furthermore, we report the first use of high throughput workflow incorporating highly parallel ball-milling and gas sorption analysis. Ball milling is a versatile technique that can synthesize a wide variety of materials in powder form from simple (often elemental) reagents on laboratory and industrial scales[19−21] and is a complementary approach to currently developed high-throughput powder synthesis tools.[5,6] It is expected that high-throughput ball-milling will find application in a number of additional areas.

EXPERIMENTAL PROCEDURES

Synthesis. All reagents were purchased and used without purification. Reagents were dispensed via automated powder-handling tools installed within a recirculating argon-filled glovebox (O_2, H_2O < 3 ppm). Reagents were loaded (typical total mass ∼300 mg) into hardened tool steel reaction wells with chrome-steel milling media. Once loaded, the wells were sealed, removed from the glovebox and charged with 20 bar He to provide overpressure protection against small leaks. Materials were milled at high energy for a total of 24 h. Variations in synthetic conditions were attempted (lower acceleration and shorter milling times) but the materials so-synthesized exhibited inferior initial rates per the primary screen. The additives and additive combinations tested are detailed in Figure 3 and Supporting Information, Figures S2 and S3. For all reactions the amount of each reagent is detailed as $2LiNH_2$:$1MgH_2$ + xA where x is the molar percentage of the total molar amount; that is, $100\%{\cdot}x/(3 + x)$.

Analysis. All sorption analyses detailed herein were performed using our custom parallel volumetric gas-sorption instruments. Each instrument contains 28 channels equipped with independent pressure sensors and manifold volumes. Prior to use, each instrument was calibrated and validated with blank sample holders and palladium foil. Furthermore, samples including $LaNi_5$, TiFe, and $2LiNH_2$:MgH_2 + 5 at % $LiBH_4$ + 1 at % La + 5 at % Li_3N were analyzed on both our instrument and a Hy-Energy PCT-Pro 2000, yielding identical results within 0.2 wt %. In addition, we ball-milled a sample of $2LiNH_2$:MgH_2 + 15 at % Si that we measured ourselves and sent for measurement by Karl Gross of Hy-Energy, LLC on a PCT-Pro 2000. Shown in Supporting Information, Figure S8 is the excellent agreement obtained. For all data within this paper, hydrogen absorption is wt % of the total loaded reagent mass; that is, mass H_2 absorbed/(mass of $2LiNH_2$ + MgH_2 + xA). This is equivalent to wt % when the additive is either fully hydrided (like $LiNH_2$ and MgH_2) or when the additive has no hydrogen capacity. Overestimates in wt % occur when the additive has hydrogen capacity but is added in the dehydrided state: the amount absorbed by the additive is not included in the denominator. The largest possible error during primary screening (Figure 2) is 0.3 percentage points (for Li_3N) and 0.1 percentage points for the compounds characterized in Figures 4 and 5.

Data in Figures 1−4 were obtained via the primary screen protocol. In this measurement, prior to desorbing the system, the free space volume was measured at room temperature and a temperature correction applied to obtain the free space at 150 °C. The maximum expected error in the measured free space deriving from the change in sample volume upon dehydrogenation is $\sim 10^{-4}$ mL ($\ll$ 1%). The temperature correction was obtained by analyzing blank sample holders with the same analysis protocol. Data in Figures 4 and 5, and Supporting

dx.doi.org/10.1021/co2001789 | ACS Comb. Sci. 2012, 14, 352−358

Information, Figures S4, S5, and S6 were obtained on our instrument from the same 11-cycle run. Prior to each absorption measurement, the materials were degassed for 15 h at 150 °C under dynamic vacuum. The sample volume was then cooled to 120 °C and exposed to approximately 45 bar hydrogen for 6 h. The free space was measured with He at 120 °C prior to the first absorption and used for all subsequent cycles. A background correction was applied to each cycle by subtracting the pressure drop observed for blank sample holders (equivalent to 0.4−0.6 wt % in 6 h). Repeat synthesis and measurements of interesting materials showed standard deviations less than 5%.

Electron micrographs (Supporting Information, Figure S6) were obtained with a JEOL JSM 6390 SEM-EDS system.

■ ASSOCIATED CONTENT

Supporting Information

Additional plots of absorption data and electron microscopy image. This material is available free of charge via the Internet at http://pubs.acs.org.

■ AUTHOR INFORMATION

Corresponding Author

*E-mail: mbailey@kinestral.com.

Notes

The authors declare no competing financial interest.

■ ACKNOWLEDGMENTS

We thank P. G. Schultz, D. W. Murphy, and R. Russo for advice and discussion. We thank R. C. Downs, K. Micklash, I. Lopez, J. Dutton, and P. Ziegelbauer for help with the design and the construction of the high throughput workflow.

■ REFERENCES

(1) Yang, J.; Sudik, A.; Wolverton, C.; Siegel, D. J. High Capacity Hydrogen Storage Materials: Attributes for Automotive Applications and Techniques for Materials Discovery. *Chem. Soc. Rev.* **2010**, *39*, 656−675.

(2) Orimo, S.-I.; Nakamori, Y.; Eliseo, J. R.; Züttel, A.; Jensen, C. M. Complex Hydrides for Hydrogen Storage. *Chem. Rev.* **2007**, *107*, 4111−4132.

(3) Eberle, U.; Felderhoff, M.; Schüth, F. Chemical and Physical Solutions for Hydrogen Storage. *Angew. Chem., Int. Ed.* **2009**, *48*, 6608−6630.

(4) http://www1.eere.energy.gov/hydrogenandfuelcells/storage/pdfs/targets_onboard_hydro_storage.pdf.

(5) Koinuma, H.; Takeuchi, I. Combinatorial Solid-State Chemistry of Inorganic Materials. *Nat. Mater.* **2004**, *3*, 429−438.

(6) Maier, W. F.; Stöwe, K.; Sieg, S. Combinatorial and High-Throughput Materials Science. *Angew. Chem., Int. Ed.* **2007**, *46*, 6016−6067.

(7) Alapati, S. V.; Johnson, J. K.; Sholl, D. S. Using First Principles Calculations to Identify New Destabilized Metal Hydride Reactions for Reversible Hydrogen Storage. *Phys. Chem. Chem. Phys.* **2007**, *9*, 1438−1452.

(8) Wolverton, C.; Siegel, D. J.; Akbarzadeh, A. R.; Ozoliņš, V. Discovery of Novel Hydrogen Storage Materials: An Atomic Scale Computational Approach. *J. Phys.: Condens. Matter* **2008**, *20*, 064228.

(9) Olk, C. H.; Tibbets, G. G.; Simon, D.; Moleski, J. J. Combinatorial Preparation and Infrared Screening of Hydrogen Sorbing Metal Alloys. *J. Appl. Phys.* **2003**, *94*, 720−725.

(10) Dam, B.; Gremaud, R.; Broedersz, C.; Griessen, R. Combinatorial Thin Film Methods for the Search of New Lightweight Metal Hydrides. *Scripta Materialia* **2007**, *56*, 853−858.

(11) Gremaud, R.; Broedersz, C. P.; Borsa, D. M.; Borgschulte, A.; Mauron, P.; Schreuders, H.; Rector, J. H.; Dam, B.; Griessen, R. Hydrogenography: An Optical Combinatorial Method to Find New Light-Weight Hydrogen Storage Materials. *Adv. Mater.* **2007**, *19*, 2813−2817.

(12) Guerin, S.; Hayden, B. E.; Smith, D. C. A. High-Throughput Synthesis and Screening of Hydrogen-Storage Alloys. *J. Comb. Chem.* **2008**, *10*, 37−43.

(13) Amieiro-Fonseca, A.; Ellis, S. R.; Nuttall, C. J.; Hayden, B. E.; Guerin, S.; Purdy, G.; Soulié, J.-Ph.; Callear, S. K.; Culligan, S. D.; David, W. I. F.; Edwards, P. P.; Jones, M. O.; Johnson, S. R.; Pohl, A. H. A Multidisciplinary Combinatorial Approach for Tuning Promising Hydrogen Storage Materials Towards Automotive Applications. *Faraday Discuss.* **2011**, *151*, 369−384.

(14) Barcelo, S.; Mao, S. High Throughput Optical Characterization of Alloy Hydrogenation. *Int. J. Hydrogen Energy* **2010**, *35*, 7228−7231.

(15) Oguchi, H.; Heilweil, E. J.; Josell, D.; Bendersky, L. A. Infrared Emission Imaging as a Tool for Characterization of Hydrogen Storage Materials. *J. Alloys Compd.* **2009**, *477*, 8−15.

(16) Cao, L. R.; Hattrick-Simpers, J. R.; Bindel, R.; Tomlin, B. E.; Zeisler, R.; Paul, R.; Bendersky, L. A.; Downing, R. G. Combinatorial Study of Thin Film Metal Hydride by Prompt Gamma Activation Analysis. *J. Radioanal. Nucl. Chem.* **2010**, *283*, 63−68.

(17) Lewis, G. J.; Sachtler, J. W. A.; Low, J. J.; Lesch, D. A.; Faheem, S. A.; Dosek, P. M.; Knight, L. M.; Halloran, L.; Jensen, C. M.; Yang, J.; Sudik, A.; Siegel, D. J.; Wolverton, C.; Ozolins, V.; Zhang, S. High Throughput Screening of the Ternary $LiNH_2$-MgH_2-$LiBH_4$ Phase Diagram. *J. Alloys Compd.* **2007**, *446*−*447*, 355−359.

(18) http://www.hydrogen.energy.gov/pdfs/review06/st_14_zhao.pdf.

(19) Suryanarayana, C. Mechanical Alloying and Milling. *Prog. Mater. Sci.* **2001**, *46*, 1−184.

(20) Suryanarayana, C. Recent Developments in Mechanical Alloying. *Rev. Adv. Mater. Sci.* **2008**, *18*, 203−211.

(21) Baláž, P. *Mechanochemistry in Nanoscience and Minerals Engineering*; Springer-Verlag: Berlin, Germany, 2008.

(22) Koch, C. C.; Whittenberger, J. D. Mechanical Milling/Alloying of Intermetallics. *Intermetallics* **1996**, *4*, 339−355.

(23) Tan, G. L.; Wu, N.; Zheng, J. G.; Hommerich, U.; Temple, D. Optical Absorption and Valence Band Photoemission from Uncapped CdTe Nanocrystals. *J. Phys. Chem. B* **2006**, *110*, 2125−2130.

(24) Asano, K.; Enoki, H.; Akiba, E. Synthesis of HCP, FCC, BCC Structure Alloys in the Mg-Ti Binary System by Means of Ball Milling. *J. Alloys Compd.* **2009**, *480*, 558−563.

(25) Tarascon, J.-M.; Morcrette, M.; Saint, J.; Aymard, L.; Janot, R. On the Benefits of Ball Milling Within the Field of Rechargeable Li-Based Batteries. *C. R. Chim.* **2005**, *8*, 17−26.

(26) Ning, L. J.; Wu, Y. P.; Fang, S. B.; Rahm, E.; Holze, R. Materials Prepared for Lithium Ion Batteries by Mechanochemical Methods. *J. Power Sources* **2004**, *133*, 229−242.

(27) Yang, X. G.; Wang, C. Y. Nanostructured Tungsten Carbide Catalysts for Polymer Electrolyte Fuel Cells. *Appl. Phys. Lett.* **2005**, *86*, 224104.

(28) Lan, Y.; Minnich, A. J.; Chen, G.; Ren, Z. Enhancement of Thermoelectric Figure-of-Merit by a Bulk Nanostructured Approach. *Adv. Funct. Mater.* **2010**, *20*, 357−376.

(29) James, S. L.; Adams, C. J.; Bolm, C.; Braga, D.; Collier, P.; Friščić, T.; Grepioni, F.; Harris, K. D. M.; Hyett, G.; Jones, W.; Krebs, A.; Mack, J.; Maini, L.; Orpen, A. G.; Parkin, I. P.; Shearouse, W. C.; Steed, J. W.; Waddell, D. C. Mechanochemistry: Opportunities for New and Cleaner Synthesis. *Chem. Soc. Rev.* **2012**, *41*, 413−447.

(30) Luo, W. ($LiNH_2$-MgH_2): A Viable Hydrogen Storage System. *J. Alloys Compd.* **2004**, *381*, 284−287.

(31) Xiong, Z.; Wu, G.; Hu, J.; Chen, P. Ternary Imides for Hydrogen Storage. *Adv. Mater.* **2004**, *16*, 1522−1525.

(32) Xiong, Z.; Hu, J.; Wu, G.; Chen, P.; Luo, W.; Gross, K.; Wang, J. Thermodynamic and Kinetic Investigations of the Hydrogen Storage in the Li-Mg-N-H System. *J. Alloys Compd.* **2005**, *398*, 235−239.

(33) Luo, W.; Wang, J.; Stewart, K.; Clift, M.; Gross, K. Li-Mg-N-H: Recent Investigations and Development. *J. Alloys Compd.* **2007**, *446*−*447*, 336−341.
(34) Liu, Y.; Zhong, K.; Luo, K.; Gao, M.; Pan, H.; Wang, Q. Size-Dependent Kinetic Enhancement in Hydrogen Absorption and Desorption of the Li-Mg-N-H System. *J. Am. Chem. Soc.* **2009**, *131*, 1862−1870.
(35) $Li_2Mg(NH)_2$ is the dehydrided form of reaction 1, and can be synthesized either by dehydriding the reaction product of 2LiH + $Mg(NH_2)_2$ or 2$LiNH_2$ + MgH_2. Once $Li_2Mg(NH)_2$ is formed, the hydriding and dehydriding occurs per reaction 1.
(36) Yang, J.; Sudik, A.; Siegel, D. J.; Halliday, D.; Drews, A.; Carter, R. O.; Wolverton, C.; Lewis, G. J.; Adriaan Sachtler, J. W.; Low, J. J.; Faheem, S. A.; Lesch, D. A.; Ozolins, V. A Self-Catalyzing Hydrogen-Storage Material. *Angew. Chem., Int. Ed.* **2008**, *47*, 882−887.
(37) Hu, J.; Liu, Y.; Wu, G.; Xiong, Z.; Chua, Y. S.; Chen, P. Improvement of Hydrogen Storage Properties of the Li-Mg-N-H System by Addition of $LiBH_4$. *Chem. Mater.* **2008**, *20*, 4398−4402.
(38) Sudik, A.; Yang, J.; Halliday, D.; Wolverton, C. Hydrogen Storage Properties in $(LiNH_2)_2$-$LiBH_4$-$(MgH_2)_x$ Mixtures (x = 0.0−1.0). *J. Phys. Chem. C* **2008**, *112*, 4384−4390.
(39) Hu, J.; Fichtner, M.; Chen, P. Investigation on the Properties of the Mixture Consisting of $Mg(NH_2)_2$, LiH, and $LiBH_4$ as a Hydrogen Storage Material. *Chem. Mater.* **2008**, *20*, 7089−7094.
(40) Sudik, A.; Yang, J.; Halliday, D.; Wolverton, C. Kinetic Improvement in the $Mg(NH_2)_2$-LiH Storage System by Product Seeding. *J. Phys. Chem. C* **2007**, *111*, 6568−6573.
(41) Ma, L.-P.; Fang, Z.-Z.; Dai, H.-B.; Kang, X.-D.; Liang, Y.; Wang, P.-J.; Wang, P.; Cheng, H.-M. Effect of Li_3N Additive on the Hydrogen Storage Properties of Li-Mg-N-H System. *J. Mater. Res.* **2009**, *24*, 1936−1942.
(42) Liang, C.; Liu, Y.; Jiang, Y.; Wei, Z.; Gao, M.; Pan, H.; Wang, Q. Local Defects Enhanced Dehydrogenation Kinetics of the $NaBH_4$-added Li-Mg-N-H System. *Phys. Chem. Chem. Phys.* **2011**, *13*, 314−321.
(43) Ma, L.-P.; Dai, H.-B.; Liang, Y.; Kang, X.-D.; Fang, Z.-Z.; Wang, P.-J.; Wang, P.; Cheng, H.-M. Catalytically Enhanced Hydrogen Storage Properties of $Mg(NH_2)_2$ + 2LiH Material by Graphite-Supported Ru Nanoparticles. *J. Phys. Chem. C* **2008**, *112*, 18280−18285.
(44) Wang, J.; Hu, J.; Liu, Y.; Xiong, Z.; Wu, G.; Pan, H.; Chen, P. Effects of Triphenyl Phosphate on the Hydrogen Storage Performance of the $Mg(NH_2)_2$-2LiH System. *J. Mater. Chem.* **2009**, *19*, 2141−2146.
(45) Zhang, X.; Li, Z.; Lu, F.; Li, H.; Mi, J.; Wang, S.; Liu, X.; Jiang, L. Improved Hydrogen Storage Performance of the $LiNH_2$-MgH_2-$LiBH_4$ System by Addition of ZrCo Hydride. *Int. J. Hydrogen Energy* **2010**, *35*, 7809−7814.
(46) Wang, J.; Liu, T.; Wu, G.; Li, W.; Liu, Y.; Moysés Araújo, C.; Scheicher, R. H.; Blomqvist, A.; Ahuja, R.; Xiong, Z.; Yang, P.; Gao, M.; Pan, H.; Chen, P. Potassium-Modified $Mg(NH_2)$/2LiH System for Hydrogen Storage. *Angew. Chem., Int. Ed.* **2009**, *48*, 5828−5832.
(47) Vajo, J. J.; Olson, G. L. Hydrogen Storage in Destabilized Chemical Systems. *Scr. Mater.* **2007**, *56*, 829−834.
(48) Johnson, S. R.; Anderson, P. A.; Edwards, P. P.; Gameson, I.; Prendergast, J. W.; Al-Mamouri, M.; Book, D.; Harris, I. R.; Speight, J. D.; Walton, A. Chemical Activation of MgH_2: A New Route to Superior Hydrogen Storage Materials. *Chem. Commun.* **2005**, 2823−2825.
(49) Bérubé, V.; Radtke, G.; Dresselhaus, M.; Chen, G. Size Effects on the Hydrogen Storage Properties of Nanostructured Metal Hydrides: A Review. *Int. J. Energy Res.* **2007**, *31*, 637−663.
(50) Two sequential desorption/absorption cycles were run for every reaction set containing additives with the potential to absorb hydrogen.
(51) David, W. I. F.; Jones, M. O.; Gregory, D. H.; Jewell, C. M.; Johnson, S. R.; Walton, A.; Edwards, P. P. A Mechanism for Non-Stoichiometry in the Lithium Amide/Lithium Imide Hydrogen Storage Reaction. *J. Am. Chem. Soc.* **2007**, *129*, 1594−1601.
(52) Rijssenbeek, J.; Gao, Y.; Hanson, J.; Huang, Q.; Jones, C.; Toby, B. Crystal Structure Determination and Reaction Pathway of Amide-Hydride Mixtures. *J. Alloys Compd.* **2008**, *454*, 233−244.